Spectral measurements of inductively coupled and m = +1, −1 helicon discharge modes of the constructed plasma source

Mohammadreza Khoshhal (iD), Morteza Habibi (iD), and Rod Boswell

COLLECTIONS

Paper published as part of the special topic on Chemical Physics, Energy, Fluids and Plasmas, Materials Science and Mathematical Physics

View Online   Export Citation   CrossMark

ARTICLES YOU MAY BE INTERESTED IN

Three-dimensional measurements of fundamental plasma parameters in pulsed ICP operation
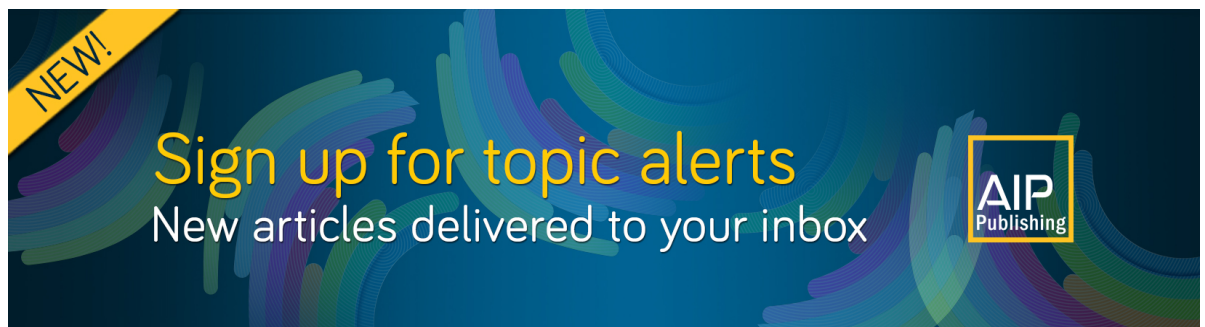Physics of Plasmas **27**, 063509 (2020); https://doi.org/10.1063/5.0007288

Effect of electron kinetics on plasma density in inductively coupled plasmas using a passive resonant antenna
Physics of Plasmas **27**, 063511 (2020); https://doi.org/10.1063/5.0006698

Modification of momentum flux lost to a radial wall of a helicon source by neutral injection
Physics of Plasmas **27**, 064504 (2020); https://doi.org/10.1063/5.0002173

Spectral measurements of inductively coupled and m = +1, −1 helicon discharge modes of the constructed plasma source

View Online   Export Citation   CrossMark

Mohammadreza Khoshhal,[1,a] (iD)   Morteza Habibi,[1] (iD) and Rod Boswell[2]

AFFILIATIONS

[1] Helicon Plasma Laboratory, Department of Energy Engineering and Physics, Amirkabir University of Technology-Tehran Polytechnic, 159163-4311 Tehran, Iran
[2] Space Plasma, Power and Propulsion Laboratory, Research School of Physics and Engineering, The Australian National University, Canberra, Australian Capital Territory 2601, Australia

[a] Author to whom correspondence should be addressed: m.khoshhal@aut.ac.ir

ABSTRACT

In the present context, the industrial type of Amirkabir helicon plasma source has been introduced that was designed and constructed at the Helicon Plasma Laboratory of Amirkabir University of Technology with the aim of using it in material processing applications. Helicon plasma in two m = +1 and m = −1 modes of operation was studied, and also its application was compared with the inductively coupled plasma (ICP) mode in this experimental work. This study was performed by employing two techniques including optical emission spectroscopy and imaging using a camera with polarizing filters, in which the images and spectra of ICP and m = +1, −1 helicon plasma modes were recorded under the experimental conditions. The effects of the device operational parameters on the argon plasma emission spectra were investigated in the wavelength range of 350–950 nm. It was observed from the comparison of the plasma spectra that the ionization rate increases significantly for the plasma helicon mode than ICP and also for m = +1 helicon mode of operation than m = −1. In this work, the values of device operational parameters such as the RF power delivered to the half-helix antenna, external magnetic field intensity, and the injected gas flow rate were varied in the range of 400–900 W, 100–300 mT, and 1–10 SCCM in the experiment, respectively. In addition, the optimum values of RF power, magnetic field intensity, and the injected gas flow rate for achieving the maximum ionization rate were, respectively, obtained as 900 W, 300 mT, and 3 SCCM.

I. INTRODUCTION

Helicon waves have been studied in two aspects of theories[1,2] and experiments,[3,4] which were carried out in gas and solid plasmas.

The new era of helicon wave investigation began when Boswell[3,5] successfully used helicon waves for the generation of high density plasma (∼4 × 10^{18} m^{-3}) in a cylindrical glass tube in a 75 mT axial magnetic field at the applied 600 W RF power. This valuable work leads to the generation of plasma that has at least an order increased density than the RF conventional plasmas under the same power conditions.[6–9]

Helicon plasma sources have been used in a wide range of industrial applications,[10] including high beta studies,[11,12] material processing,[13] and plasma propulsion.[14–16] A plasma source consists of the important parts such as an antenna for power transition, magnets for the generation of axial magnetic field, and a cylindrical quartz tube as the plasma vessel and gas injection system. Using a helical shaped radio frequency antenna for high density plasma generation has been extensively studied. In the Inductively Coupled Plasma (ICP) sources, a helical shaped coil surrounding plasma generation region generates a time-varying magnetic field when it is supplied by RF currents. The generation of this magnetic field in the mentioned region leads to the induction of the solenoidal RF

electric field that causes acceleration of free electrons and plasma formation.[1]

In helicon plasma sources, similar to what happened in ICP, an RF helical antenna surrounding a dielectric cylindrical vessel excites a helicon wave within the plasma source by Direct Current (DC) axial magnetic field that is applied in the plasma generation region.[1] Concerning a selective excitation of the azimuthal mode number m, some examples of various RF antenna that are utilized in the helicon plasma source include single or multi-loops[17] for the m = 0 mode; double saddle[18] (the Boswell type) for both m = ±1 modes; the Nagoya type III antenna[19] for the m = +1 or −1 mode depending on the RF phase between leg currents and the half or full helical type[20] for the m = +1 or −1 mode depending on the direction of the axial magnetic field and/or the twisting direction. However, the half-helix type was employed specifically to enable m = +1 and m = −1 modes of operation for this study in order to investigate the effect of the magnetic field on helicon plasma ionization.[20–25]

The jump to the helicon mode has always been associated with a significant increase in plasma density and also formation of a radially localized central region of very strong ion light emission known as the bright core.

The appearance of the blue core in which the central volume of the plasma turns light blue due to emission of ArII lines is typically considered as an identification of the helicon mode in argon plasma that can be recorded by using a camera with polarizing filters.[26–28]

The laboratory type of Amirkabir Helicon Plasma Source (AHPS-I), which was constructed with the aim of using in the related research to helicon plasma, has a Nagoya-III antenna employed for helicon wave excitation with an axial magnetic field intensity 350 G that could maintain helicon plasma just for up to 90 s.[29]

In this work, the novel AHPS-II was designed and constructed in which the discharge regime change from the H-mode (ICP) to the W-mode (helicon) was analyzed by employing Optical Emission Spectroscopy (OES) over the range of 350–950 nm.[8,9,26] In addition, three main operational parameters of the device including the external magnetic field, the gas flow rate, and the RF power delivered to the antenna were optimized for achieving the maximum ionization rate.

Our main purpose of design and construction of this helicon plasma source is to employ it in industrial applications such as material processing and ion implantation. This study approaches the analysis of the device operational parameter effect on the ionization rate in two helicon modes (m = +1, −1), especially for low RF powers, which can be beneficial for the construction and optimization of the efficient industrial helicon plasma sources.

This paper outlines the theoretical background in Sec. II, experimental setup and procedures in Sec. III, results and discussion in Sec. IV, analysis of plasma regime change from ICP to m = +1, −1 helicon modes in Sec. IV A, observations of the operational parameter scans in Sec. IV B, and finally, our results have been concluded in Sec. V.

II. THEORETICAL BACKGROUND

Helicons are propagating wave modes in a cylindrically confined, axially magnetized plasma column. These modes, which have electric and magnetic fields with radial, axial and, usually, azimuthal

variation, propagate in low frequency, low magnetic field, and high density regime characterized by $\omega_{LH} \ll \omega \ll \omega_{ce}$ and $\omega_{pe}^2 \gg \omega\omega_{ce}$, where ω_{LH}, ω, ω_{ce}, and ω_{pe} are the lower hybrid frequency, driving frequency, electron cyclotron frequency, and electron plasma frequency, respectively.[30]

The dispersion relation for uniform plasma by neglecting the dissipation reduces to the classic relation for low frequency whistler waves,

$$\omega = kk_\parallel B_0/en_0\mu_0, \tag{1}$$

in which $k^2 = |k|^2 = k_\perp^2 + k_\parallel^2$, k is the wave vector, $k_\perp$ and $k_\parallel$, respectively, the perpendicular and parallel wave numbers, B_0 is the DC magnetic field, and n_0 is the electron density.

The values of $k_\perp$ and $k_\parallel$ were set by boundary condition that mainly differ a little in cases m = +1 and m = −1 waves. There are considerable differences in excitation of m = +1, m = −1 modes that were shown in calculations including antenna coupling, plasma inhomogeneity, and damping.[31,32]

The linear helicon waves generally have circularly polarized eigenmodes with electric fields varying as

$$E = B, \quad E(r)\exp[i(m\theta + kz - \omega t)], \tag{2}$$

in which m, k, and θ are the azimuthal mode number, wave number, and azimuthal angle, respectively.[33]

Considering the adopted sign convention, the positive and negative k values, respectively, denote propagation in $B_0\hat{z}$ and the opposite direction.

The positive m means the θ value increases with time, and if viewed along B_0, for an unvaried z, the vectors rotate clockwise at time, which is known as right-hand polarization. Thus, the negative m indicates the left-hand polarization. In addition, a right-hand wave (m = +1) can have either positive or negative helicity regarding the k direction.

When a wave moves in the +z direction (k > 0) and a stationary observer looking along z, the vectors are observed to rotate clockwise that is considered as the right-hand polarized wave. On the other hand, if the waveform moves in the −z direction (k < 0), we have a left-hand (m = −1) wave.

As a result, a waveform with m/k < 0 can represent either a right-hand wave moving in the −z direction or a left-hand wave
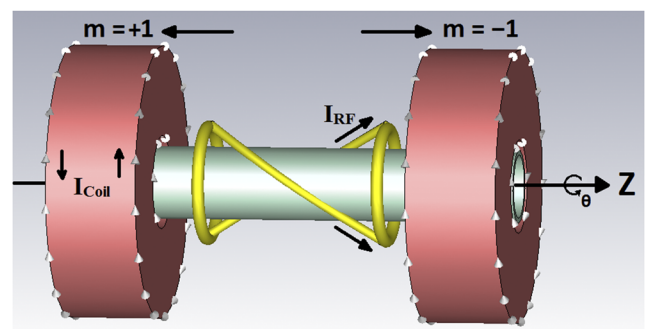

FIG. 1. 3D configuration of the helicon plasma source analyzed half-helix antenna for m = +1 and m = −1 wave excitations; simulated by finite element method (FEM) based CST Studio Suite software.

propagating in +z direction.[22,34] Figure 1 shows the 3D configuration of the helicon plasma source analyzed half-helix antenna for m = +1 and m = −1 wave excitation that was simulated by the finite element method (FEM) based CST Studio Suite software.

In the previous research works, a half-helix antenna was employed to launch both of m = +1 and m = −1 waves separately by reversing the imposed magnetic field (B_0) direction.[20,25,35–37]

III. EXPERIMENTAL SETUP AND PROCEDURES

Different parts of the constructed plasma source, the procedure of project implementation, and the method of spectroscopy process have been mentioned in this section. All the plasma source construction steps and spectral measurements were conducted in the Helicon Plasma Laboratory of AUT. The schematic of the experimental setup of the AHPS-II, measurement and diagnostic devices, and cooling systems are shown in Fig. 2. The AHPS-II was designed for industrial applications and can be employed to work in a continuous state.

As shown in Fig. 2, the water cooling system was designed and constructed for cooling the both antenna and diffusion pump. In addition, the gas cooling system was provided for cooling the electromagnets.

In this study, three operational parameters of AHPS-II including the RF power, the external magnetic field, and the injected argon gas flow rate were investigated, respectively, in the ranges of 400–900 W, 100–300 mT, and 1–10 SCCM.

A. The plasma source

The constructed helicon plasma source (Fig. 3) consists of a cylindrical quartz tube, which is considered as the plasma chamber, which its length and diameter is 50 cm and 5 cm, respectively. Two gas-cooled cylindrical electromagnets were designed and constructed that surround this plasma chamber. In addition, a water-cooled half-helix antenna, which was constructed of copper, was placed between these two electromagnets outside the plasma chamber. The image of the constructed plasma source is shown in Fig. 3.

The plasma chamber from one end was connected to a propellant gas flow line. The gas flow is controlled by a digital flowmeter. This flowmeter (Fig. 2) injects a determined gas flow to the plasma chamber through a 316 stainless steel tube. In this study, the experiments were performed using argon gas.

The electromagnets, which are in Helmholtz configuration, provide helicon discharge. The maximum strength of the generated axial magnetic fields in the center of electromagnets for the 100 A current is obtained equal to 300 mT. Figure 4 shows the image of the constructed electromagnets.

Since it is not possible to change the applied current values to electromagnets, and also for the generation of magnetic fields with different intensities, the coils were designed in a way that enable us to get access to the different turn numbers of wire. Each electromagnet, thus, has four inputs for DC current imposing (Fig. 4). These inputs regarding which couple of those is chosen for current imposing can enable the user to have access the specific wire turn numbers (N). For a better description of the operational mechanism of the constructed electromagnets, the simulated coil with these four inputs and also the introduction of just four different cases of current imposing, designed by using CST Studio, were shown in Fig. 5.

As observed in Fig. 5, for instance, if the current supply outputs are connected to the first and the second inputs of the electromagnet, the supply current is merely imposed to 300 turns of coil of 1800 possible turns. Table I shows the five different cases of current imposing
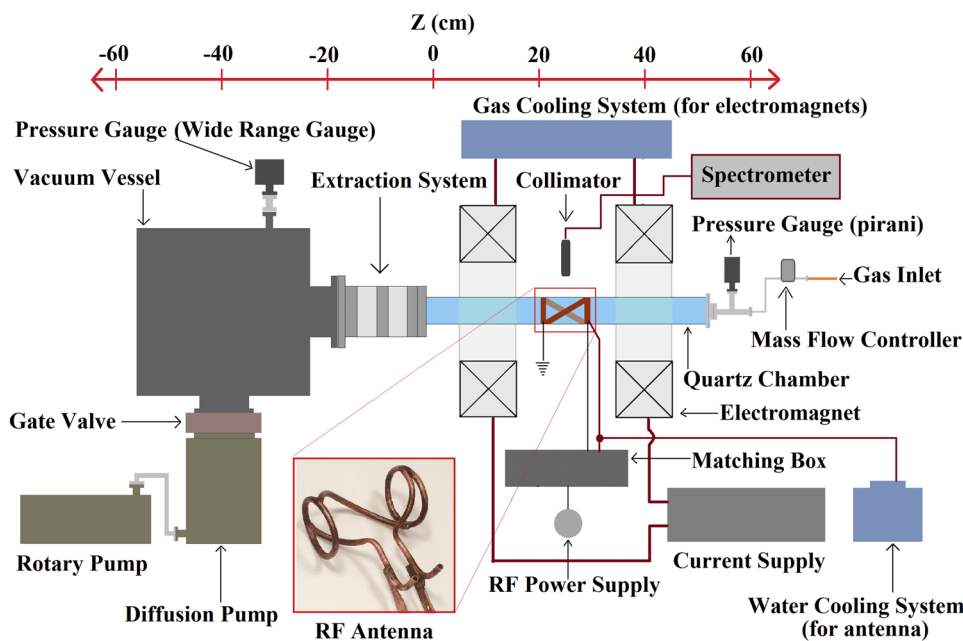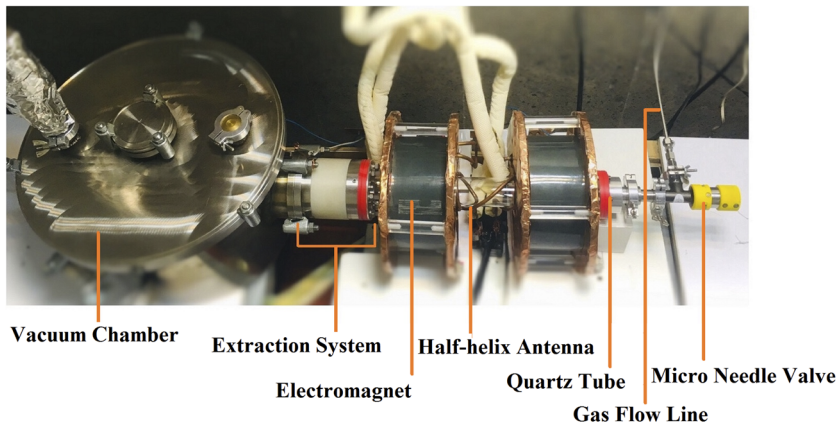

FIG. 2. The schematic of the experimental setup showing the AHPS-II.

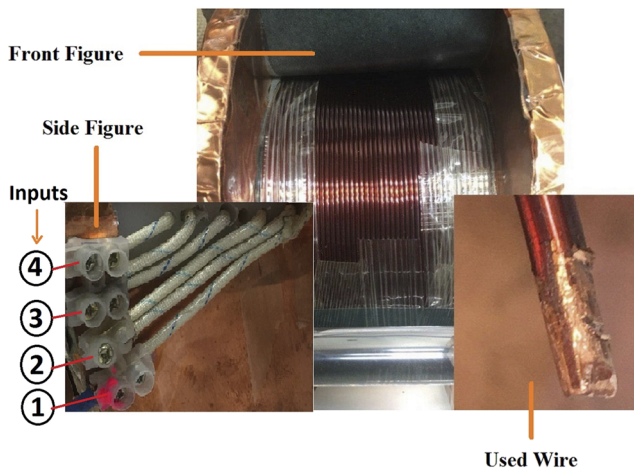**FIG. 3**. The experimental setup of the AHPS-II device constructed in the AUT Helicon Plasma Laboratory.

for four electromagnet inputs regarding the case-related specific wire turns and the obtained magnetic field.

In addition, the constructed electromagnet can be cooled by the gas-cooling system, enabling them to work efficiently in a

FIG. 4. The image of the constructed electromagnets of the AHIS-II device.

FIG. 5. The simulated electromagnet with four inputs and just four current imposing states regarding the related turning number of wire, designed by using the CST Studio.

continuous state (Fig. 2). Regarding the expected industrial applications of the constructed helicon source, this advantage, being able to work continuously, was considered for the electromagnets.

The intensity of magnetic field in the antenna region was varied by using five electromagnet inputs allowing us access the different coil turn numbers. Each input in experiments was connected to the DC 100 A current supply. The generated magnetic field for each input was measured in the antenna region by using the constructed magnetic field intensity detector in which a CYSJ302C Hall Effect Sensor was employed. The magnetic field intensity, generated by the Helmholtz structural electromagnets, was varied in the range of 100–300 mT in the antenna region.
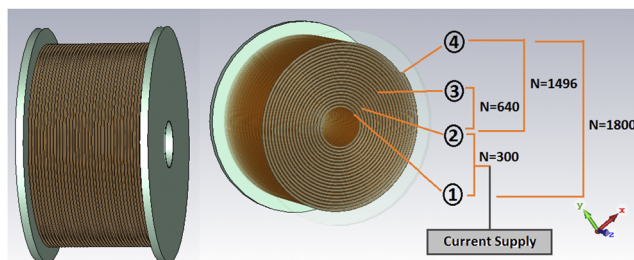
The antenna was powered by a RF supply with 2000 W power and 13.56 MHz operational frequency. The antenna was connected to a matching box, which connect the antenna to a RF power supply through a coaxial transitional line. The utilized matching box, which has the L-type circuit network, employs two adjustable vacuum and air capacitors. In addition, the antenna was constructed of a 9 mm inner diameter copper tube that can be cooled using the water-cooling system that was specially designed aiming to enable AHPS-II to operate continuously (Fig. 2).

B. Spectral measurement setup

The plasma spectroscopy technique includes collecting plasma-emitted optical spectra by using a collimator device transmitted through an optical fiber to the optical emission spectroscope (OES). A CCD detector that was provided inside the device convert the

TABLE I. Electromagnet inputs.

Input state	N (turns)	B (mT)
1–2	300	100
2–3	640	160
1–3	940	240
2–4	1496	266
1–4	1800	300

detached light to electrical signals transmitted to the computer by using a universal serial bus (USB) cable. The resulting spectra were acquired and digitally analyzed employing a C-sharp code based software suite. Figure 6 shows a schematic view of a laboratory setup employed for spectroscopy measurements.

One of the important problems in spectroscopy is the background light and its adverse effect on the quality of the received lights. Thus, a simple optical device, constructed in our lab, was used for eliminating the environment adverse lights and receiving the favorable plasma-emitted lights. This component, called the collimator, consists of two 2.5 cm diameter lens in a 10 cm focal length placed inside the opaque polyethylene cylinder. Two concentric holes of 1 cm diameter were provided at the two ends of the collimator. The collected plasma emission light enters through a hole of one end and then, from the other side end connected to the optical fiber sensor, was conducted in the transitional path to the OES device.

The constructed collimator was accurately placed between the two electromagnets at a distance of 7.5 cm from the external diameter of the quartz tube, which is 45° toward bottom, and is employed for spectra collection from the plasma center.

An OPTC high resolution spectrometer V700, a spectrometer with 200–1000 measuring range, was used as the dispersive instrument. This 10 cm focal length, f/3.8 aperture Czerny turner type spectrometer provides a resolution of 1.2 nm and 0.25 nm spectral accuracy in 10 μs–60 s exposure time. A SMA 905 (400 μm) NA 0.39 fiber optic connector was employed for the collected spectra transmission to the spectrometer. A Toshiba TCD1304DG CCD detector was attached to the exit port of the spectrometer for the presented spectral measurements. Dial setting is a set of adjustments related to the C-sharp OPTC spectroscopy software calibration including the speed of the spectral data transfer and plotting, number of scans and averaging, and background and trigger modes, which can be set by the user according to the specific experimental conditions.

Furthermore, a tungsten lamp with the determined continuum emission intensity was used for the calibration of the measured spectra intensities. The tungsten lamp in the calibration test was precisely placed in the same location of the plasma source. For the intensity measurement of tungsten lamp-emitted emission, we use the same light path and exposer time for each spectrometer dial setting that was determined for taking helicon plasma emission data.

C. Spectral measurement procedure

The vacuum pressure level in vacuum and the plasma chamber by using two diffusion and rotary pumps was obtained, respectively, 3×10^{-6} mbar and 2×10^{-4} mbar before the plasma source starts to work (Fig. 2).

First, the argon gas with a specific current value, determined by using a digital flowmeter, was injected to the plasma chamber through a 316 stainless steel pipe as a gas flow line (Fig. 3).

The background pressure within the plasma vessel, for 1 SCCM argon gas flow rate, was stabilized around 7×10^{-4} mbar.

Second, the RF power supply and matching box were triggered after turning on the cooling system of the antenna, magnets, and matching box (Fig. 2). The argon plasma discharge under conditions in which vacuum and air capacitors in the matching box have been adjusted, and can be observed at 50 W power.

Then, by increasing the power values and achieving the inductive mode, the 100 A current supply was triggered; therefore, the generated currents were delivered to the wires of electromagnets. The electromagnet inputs help us have an appropriate intensity of the magnetic field in the antenna region between the electromagnets. Imposing an external magnetic field make us closer to achieve appropriate helicon plasma. Our observations of plasma brightness and stability help us obtain the best match by adjusting the vacuum and air capacitor; therefore, the reflective power value in this case will be equal to zero and the maximum power will be absorbed by the plasma. Spectral measurements are then possible for varying operational parameters.

IV. RESULTS AND DISCUSSIONS

During the experimental tests of the constructed helicon plasma source and spectral measurements, several operational parameters were varied for achieving the optimized operational mode of the plasma source by using the recorded plasma emission spectra.

RF power delivered to plasma was varied from 400 W to 900 W. Although imposing high power values up to 2000 W was provided, one of the our purposes in this work was achieving the appropriate helicon plasma in approximately low operational power values.

Corresponding to Table I in Sec. III A, there are five different states for current imposing to each electromagnet; leading to the generation of magnetic fields with different intensities regarding the
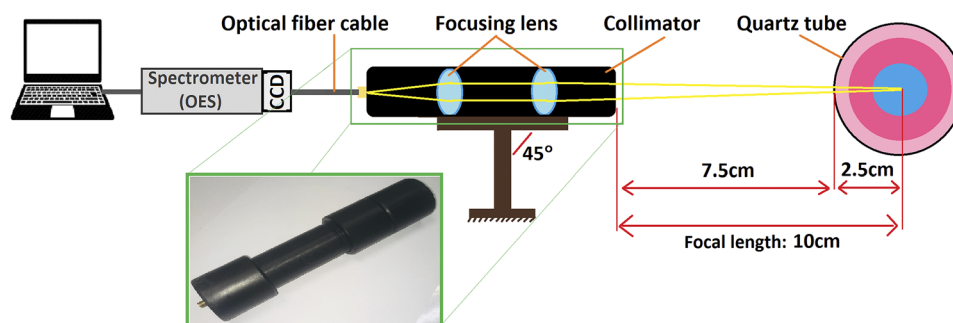

FIG. 6. The schematic view of a laboratory setup employed for spectroscopy measurements.

chosen turn number and proportionate to the provided supply current. The minimum and maximum strength of the axial magnetic field in the antenna region for 100 A DC current was obtained as 100 mT and 300 mT, respectively.

The injected argon flow rate was varied from 1 SCCM to 10 SCCM. The spectral data were recorded in the wavelength region 350–950 nm. In the study of prominent emission lines in this wavelength region, it was shown that the formed lines belong to ArI, ArII, and ArIII.

According to the NIST atomic spectra database,[38] the wavelength range of 350–500 nm was dominated by the argon single ion lines; however, the majority of the prominent emission lines in the wavelength range of 700–950 nm belong to the neutral argon atom.

A. ICP vs helicon-mode regimes

In this section, two methods including the spectral measurement using an Optical Emission Spectroscopy (OES) system installed on the AHPS-II device (Fig. 2) and photographic technique by using a camera with polarizing filters were employed for the investigation of helicon and ICP mode. In addition, using the half-helix antenna type enables us to have a logical comparison between the generated helicon plasmas in m = +1 and m = −1 helicon modes of operation.

Based on our visual observations of the generated plasma, increase in the magnetic field intensity leads to a specific difference in plasma color and emission intensity emanated from the helicon discharge. Furthermore, in the absence of an external magnetic field, which is called the inductively coupled plasma mode, no visible plume came from the plasma source. However, very bright plume was observed in entire quartz tube in both helicon modes. The helicon mode was varied from m = +1 to m = −1 by changing the imposed axial magnetic field direction with respect to the antenna current direction.

In helicon plasma sources, when argon plasma is operating in the W-mode, the color of plasma core changes from the usual red to a bright blue.[26,33,39,40] It is commonly known that the formation of a blue core in the plasma column denotes helicon wave coupling indicating W-mode operation has been achieved.[18,26,28,33,41,42] This bright core, which is produced by the intense emission from the excited argon ions (ArII) that are accelerated through the helicon wave coupling to the plasma electrons, refers to light in the blue portion of the visible spectrum.

In the photographic technique, in order to decrease the high intensity of the emission lights from the plasma and to detect the blue core of plasma, a pair of polarizing filters has been coupled to a Canon SX60HS camera. Figure 7 shows an image of plasma, which was generated in the inductively coupled mode in which the pink column of plasma can be clearly observed. In addition, the images of the generated helicon plasma in m = +1, −1 modes are shown in Fig. 8, respectively. The recorded images of helicon and inductive plasma were obtained in 900 W RF power, 300 mT magnetic field intensity, and 3 SCCM argon flow rate.

The blue core, which its formation is one of the indications of the plasma regime change from H-mode to W-mode is clearly observed in Fig. 8. In addition, when the magnetic field is turned on, the plasma column is affected by the applied magneto-static field,
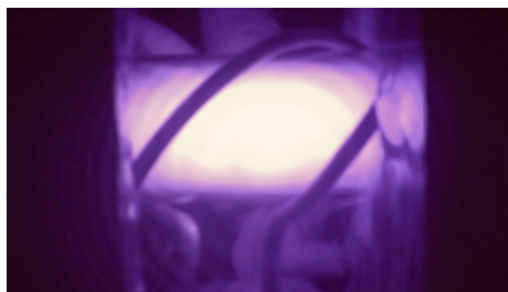

FIG. 7. The pink column of plasma generated in the ICP mode at 900 W RF power, 300 mT magnetic field intensity, and 3 SCCM argon flow rate.

leading to the appearance of a bright blue core in the center of the argon plasma column in the W-mode of operation.

Therefore, this intense blue core on the axis of the plasma column is typically used as strong identification of the helicon wave excitation in the helicon experiments at AHPS-II.

Then, by spectral measurements using the OES method, there is supporting evidence for helicon coupling that the formation of the blue core in the helicon mode is due to light emission from plasma in the wavelength region 400–500 nm.

Since the helicon wave propagates along the external magnetic field and the energy is transmitted from wave to electrons; therefore, the electrons are accelerated and their energy increases up to a point that can re-ionize ions when they collide with electrons in plasma. The ions are, thus, stimulated by their ferro-exciting due to collision with electrons, emit photons with 400–500 nm wavelength from itself leading to the formation of the blue core in the plasma column.

Figure 9 shows the comparison of high resolution emission spectra for the ICP (a), m = −1 (b), and m = +1 (c) helicon modes of operation for the argon discharge in the wavelength range of 350–950 nm at 900 W RF power, 300 mT magnetic field intensity, and 3 SCCM argon flow rate.

FIG. 8. The images of the produced blue core in m = −1 (a) and m = +1 (b) helicon modes recorded using a camera with polarizing filters at 900 W RF power, 300 mT magnetic field intensity, and 3 SCCM argon flow rate.
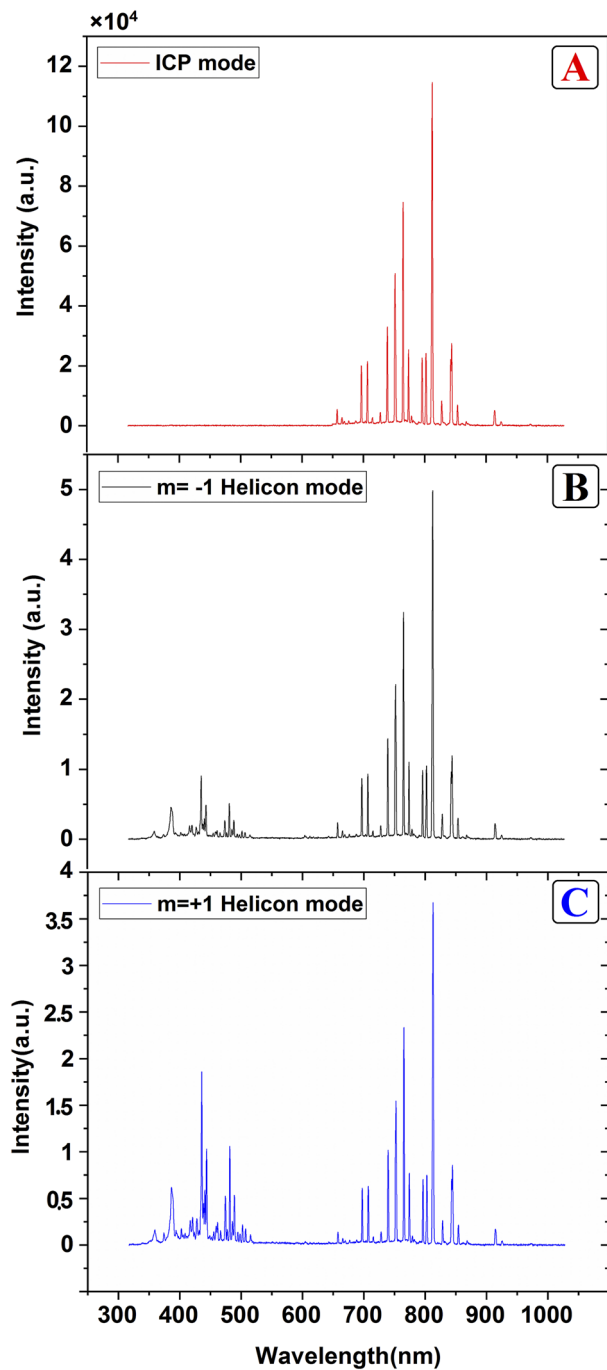
FIG. 9. The high resolution emission spectra for ICP (a) and m = −1 (b), m = +1 (c) helicon modes of operation at 900 W RF power, 300 mT magnetic field intensity, and 3 SCCM argon flow rate.

In addition, an equal exposure time and the same spectrometer dial settings were applied for each of these three tests. The current of electromagnets was turned off for the ICP mode of operation and, then, by current imposing to the electromagnets in two different directions, the argon plasma in m = +1, −1 helicon modes of operation was generated proportionate to the external axial magnetic field direction.

As seen from the graphs "B" and "C" in Fig. 9, when the magnetic field is applied, the intensity of the plasma ionic emission lines in the wavelength range of 300–550 nm region has been significantly increased. Based on the atomic spectral database (NIST[38]), the observed peaks in this region that belong to ArII can be considered as the supporting evidence for helicon coupling, and, hence, the W-mode operation has been achieved.[18,26,28,33,41,42]
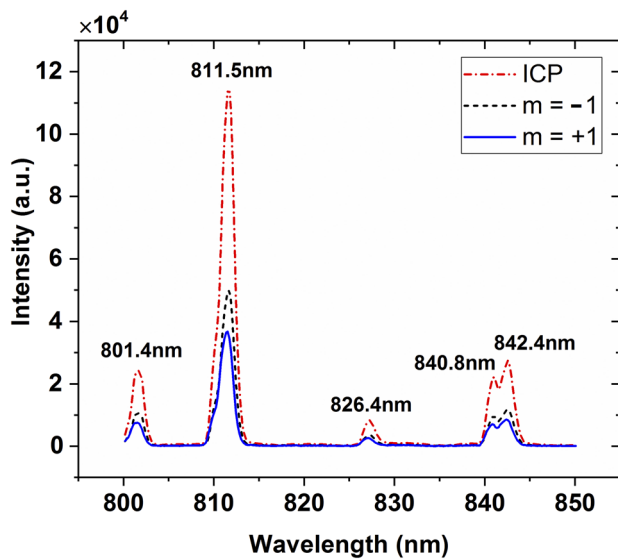
In the other words, in comparison with the ICP mode [Fig. 9(a)], the appearance of emission lines representing ArII due to the external magnetic field [Figs. 9(b) and 9(c)] can be related to the presence of electrons with minimum energy (19.5 eV), which is the required energy threshold for argon ion excitation (Ar$^+$ → Ar^{++}) within plasma, proving the helicon wave excitation and energy transmission from wave to electrons. A set of peaks obtained from the received data by OES in the wavelength range of 350–950 nm were listed in Table II based on NIST and considering the argon gas atom ionization. The AHPS-II device operational parameters for the obtained Table II data were set at 900 W RF power, 300 mT magnetic field intensity, and 3 SCCM argon flow rate.

This research specially focused on the wavelength region 800–850 nm of the spectrum, where there are only strong argon neutral emission lines, for the better comparison of the spectra that are related to the ICP mode and m = +1, −1 helicon modes of operation. The related data that were obtained in 900 W RF power, 300 mT magnetic field intensity, and 3 SCCM argon flow rate are shown in Fig. 10.

TABLE II. The argon plasma emission spectra peaks in the wavelength range of 350–950 nm at 900 W RF power, 300 mT magnetic field intensity, and 3 SCCM argon flow rate.

358.84	ArII	442.6	ArII	696.54	ArI
373.33	ArII	447.47	ArII	706.72	ArI
381.57	ArIII	454.7	ArII	714.7	ArI
385.5	ArII	458.7	ArII	727.2	ArI
390.7	ArIII	460.9	ArII	738.3	ArI
393.1	ArII	465.79	ArII	751.46	ArI
395.2	ArII	473.2	ArII	763.5	ArI
401.9	ArII	476.48	ArII	772.4	ArI
404.28	ArII	480.6	ArII	774.2	ArII
407.69	ArII	484.78	ArIII	779.5	ArII
416.25	ArII	488.22	ArII	794.8	ArI
420.06	ArI	493.6	ArII	801.4	ArI
422.98	ArII	497.21	ArII	811.5	ArI
427.21	ArI	501.49	ArII	826.4	ArI
430.9	ArII	506.2	ArII	840.8	ArI
434.8	ArII	514.53	ArII	842.4	ArI
437.92	ArII	659.6	ArI	852.1	ArI
440.09	ArII	665.35	ArII	913.8	ArII

These data were obtained under the same conditions in which the collimator was completely fixed in a specific place between electromagnets at a distance of 7.5 cm from the external diameter of the quartz tube with 45° toward the bottom in each three tests (Fig. 6).
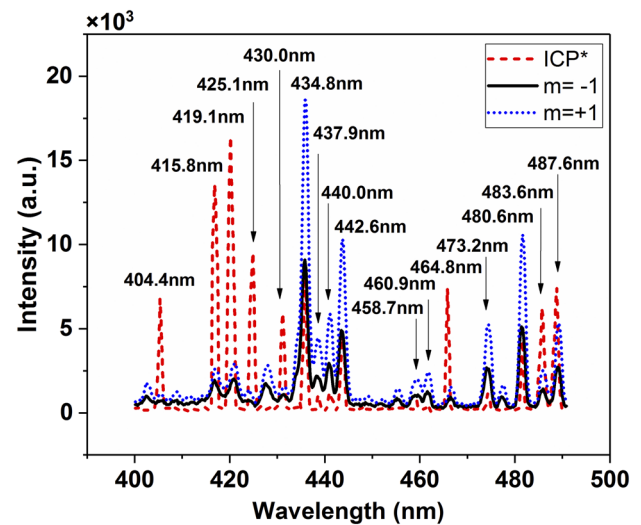
FIG. 10. The comparison of spectra related to the ICP mode and m = +1, m = −1 helicon modes of operation in the wavelength range of 800–850 nm at 900 W RF power, 300 mT magnetic field intensity, and 3 SCCM argon flow rate.

FIG. 11. The comparison of the argon plasma spectra for m = +1, −1 helicon and ICP modes of operation in wavelength range of 400–490 nm at 900 W RF power, 300 mT magnetic field intensity, and 3 SCCM argon flow rate. *The ICP spectrum is amplified 50 times.

It is observed from Fig. 10 that when separately compared with the ICP mode of operation, the emission intensity of the argon neutral lines at 801.4 nm, 811.5 nm, 826.4 nm, 840.8 nm, and 842.4 nm drops by a factor of 2.27 ± 0.03 for the m = −1 helicon mode of operation. In addition, in this figure, the emission intensity of the argon neutral lines at 801.4 nm, 811.5 nm, 826.4 nm, 840.8 nm, and 842.4 nm decreases by a factor of 1.38 ± 0.02 for the m = +1 helicon mode when compared with the m = −1 helicon mode of operation.

As seen in the graphs of the wavelength region 800–850 nm of the spectrum (Fig. 10), with the plasma regime change from the ICP to helicon mode, the neutral emission intensity drops. This can be considered as a reason of what was recorded in Figs. 7 and 8 and illuminate that why argon plasma in helicon discharge, as opposed to reddish in ICP mode, looks bright blue.

In addition, as can be observed from these graphs, while there is a low difference in the intensity of emissions in these two helicon modes in the wavelength range of 800–850 nm, which is dominated by the neutral argon atom, the emission intensity in m = −1 helicon mode is higher.

Since the effects of the magnetic field on discharge are profound, the spectral measurements that are related to the emission spectra of the antenna region in the wavelength range of 400–490 nm, obtained at 900 W RF power, 300 mT magnetic field intensity, and 3 SCCM argon flow rate, were presented in Fig. 11. As shown in the figure, the emission intensity of the prominent argon ion lines at 434.8 nm, 440 nm, 442.6 nm, 473.2 nm, and 480.6 nm increases by a factor of 116.5 ± 7.3, as the magnetic field is turned on for m = −1 helicon mode of operation. In addition, in this figure, the emission intensity of the prominent argon ion lines at 434.8 nm, 440 nm, 442.6 nm, 473.2 nm, and 480.6 nm increases by a factor

of 2.03 ± 0.07 for the m = +1 helicon mode of operation when the magnetic field direction is changed.

These comparisons make it possible to have a better quantitative estimation of how ionization varies in these three modes of operations.

In other words, the effect of the magnetic field on plasma discharge in m = +1, −1 helicon modes and ICP mode for visible electromagnetic spectra of blue portion was investigated in Fig. 11. In this figure, for a clear comparison of the ICP discharge related spectra with discharges of helicon modes, the ICP emission intensity was amplified 50 times. A few of argon neutral and single ion prominent emission lines due to ICP, m = +1 helicon, m = −1 helicon plasma modes were, respectively, identified by red, blue, and black colors.

As observed from the presented spectra in wavelength range of 400–490 nm, the argon ion prominent lines appeared in two m = +1, −1 helicon modes in which the emission intensity in the recorded plasma spectra in the right-hand helicon mode is so higher than the recorded data in the left-hand helicon mode. This can be related to the better coupling of helicon wave in the m = +1 helicon mode.[43] The condition in which the operational parameters of a plasma source including the imposed RF power, magnetic field intensity, and the injected gas flow rate were set in constant values for m = +1 and m = −1 modes of operation, the RF power absorption, ionization rate, and the population of argon single ions in m = +1 is higher than the m = −1 helicon mode,[36,43,44] leading to a significant increase in emission intensities of the single argon lines in m = +1 than m = −1 mode of operation.[25,37] In addition, regarding the ICP related amplified spectra, the neutral argon lines are more prominent in the ICP mode of operation.

The obtained results from spectral measurements, indicating the better helicon wave excitation in m = +1 helicon mode and also the higher number of ArII ions in this helicon mode, are in good

accordance with the reported previous results.[25,26,33,36,37,39,45] As discussed, the significant change in the emission spectra of the ICP and m = +1 helicon modes of operation demonstrates a sharp increase in the plasma ionization when the external magnetic field of 300 mT is provided; whereas, the comparison of variations in the emission spectra of m = +1, −1 helicon modes point out that a drop occur in plasma ionization when helicon discharge change from m = +1 to m = −1 due to change in the direction of the external magnetic field.

B. Observations of operational parameter scans

As stated earlier, several operational parameters of the plasma source were varied and the emission spectra of the generated plasma were measured in each case. The scanned parameters and their corresponding values were tabulated in Table III.

In this section, the characterization of helicon operational mode was investigated by blue core plasma intensity in two m = +1, −1 helicon modes. All the measurements discussed in this section were obtained by adjusting the impedance-matching network circuit capacity.

The prominent argon single ion emission line at 434.8 nm was identified. This prominent line was studied in order to analyze the relative strength of the obtained argon plasma.

1. Power scan

The argon plasma emission spectra were measured for m = +1, −1 helicon modes of operation as the RF power delivered to the half-helix antenna, and, hence, plasma was varied from 400 W to 900 W in 50 W increments.

The collimator device was fixed for all experiments in the antenna region for the measurement of emission spectra in the region where the discharge occurs. For these measurements, the argon gas flow rate was set in 3 SCCM, and the electromagnets were electrically connected from the fifth input state (Table I) with 1800 turns to the 100 A DC current supply. These electromagnets provide a magnetic field intensity of ~300 mT in the antenna region.

The effect of the RF power on blue core formation in helicon mode was observed. The length of the blue core, formed as a blue cylinder in the quartz tube center, increases with increase in power, whereas its diameter decreases.

Some parameters of the generated plasma in this plasma source can be better understood by the study of the specified emission line intensities. Figure 12 shows the variation in the argon single and neutral ion line emission intensities at 434.8 nm (ArII), 480.6 nm (ArII), 751.4 nm (ArI), and 763.5 nm (ArI) as the delivered RF power is varied for m = +1 helicon mode.
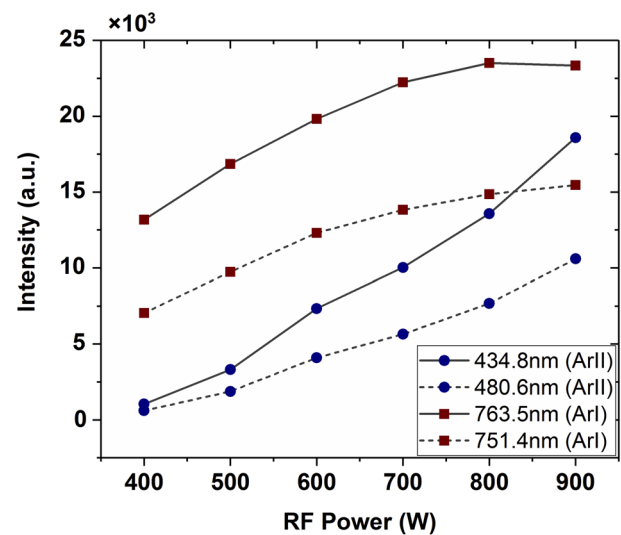

FIG. 12. The variation in the argon single and neutral ion line (Ar II: 434.8 nm, 480.6 nm and Ar I: 751.4 nm, 763.5 nm) emission intensities vs the delivered RF power for m = +1 helicon mode at 300 mT magnetic field intensity and 3 SCCM argon gas flow rate.

As observed from the graphs of Fig. 12, the argon single and neutral ion line intensities increase with the specific gradient with the increase in RF power up to 600 W. However, for the higher RF power values (>600 W), the gradient of the ArI emission lines gradually decreases, as the ArII ion line gradient increases continuously. As mentioned in Sec. IV A, the RF power increase, helicon wave coupling, and, hence, energy transition from wave to electrons (~19 eV) leading to a significant increase in ionization at plasma can be considered as another verification factor for the blue core region observed in the helicon plasma mode that have been reported by the previous researchers,[25,26,36,37,39] as one would expect by looking at the variations in the graphs of Fig. 12.

As shown in the figure, for a given set of operating conditions, including magnetic field intensity and gas flow rate, there exists an optimum RF power for neutral argon emission lines. The ion emission lines continue to rise in the power range shown. This relationship is likely due to the increase in the mean electron energy within the plasma with increasing RF power, leading to a higher fraction of electron–neutral collisions resulting in excited argon ions, rather than excited neutrals.

2. Flow rate scan

The flow rate of the gas injected to the plasma vessel was varied in the range of 1–10 SCCM, and the plasma emission spectra in a given antenna region was measured for m = +1 helicon mode. In these measurements, the delivered RF power was set at 900 W, and the electromagnets were supplied with DC 100 A current from the fifth input state (Table I) for the generation of the maximum value of the axial magnetic field up to 300 mT in the antenna region.

For the investigation of the discharge strength trends, the argon single and neutral ion emission lines at 434.8 nm (ArII), 480.6 nm

TABLE III. The plasma source operational parameter scans.

	Power (W)	Flow rate (SCCM)	B-field intensity (mT)
Power scan	400–900	3	300
Flow rate scan	900	1–10	300
B-field scan	900	3	100–300

(ArII), 751.4 nm (ArI), and 763.5 nm (ArI) were studied, and their results were shown in Fig. 13. As seen in the figure, by changing the mass flow rate, the ion emission intensity initially increases; but for the flow rate values higher than 3 SCCM, it then decreases. The percentage changes in the emission intensities for the different flow rates of 1 SCCM, 2 SCCM, 4 SCCM, 5 SCCM, 6 SCCM, 8 SCCM, and 10 SCCM, than the optimized 3 SCCM flow rate emission intensities, were, respectively, reduced by 45%, 20%, 14%, 30%, 25%, 50%, and 55%.

Therefore, there is an optimized gas flow rate for the given power level and magnetic field configuration in which the argon neutral and single ion line emission intensities reach its maximum values. Thus, it can be resulted from the figure that the ionization rate was limited to high flow rates; since the electron energy decreases with the increase in the background neutral gas density, leading to decrease in the electron temperature.[46]
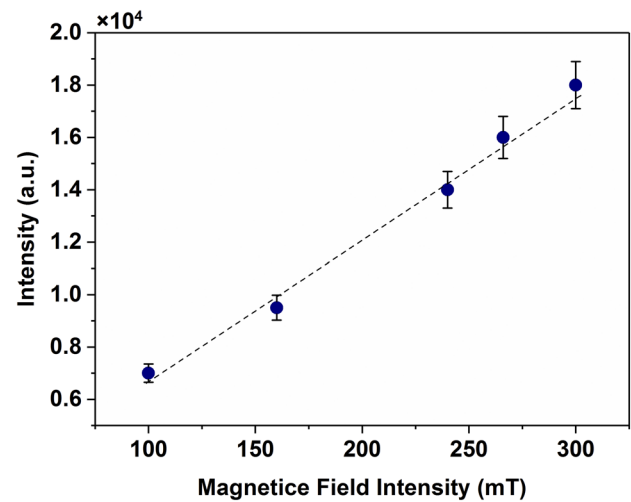
3. Magnetic field intensity scan

In this section, for the investigation of the magnetic field intensity effect on the ionization trend in helicon plasma, the magnetic field was varied in the range of 100–300 mT in which the RF power delivered to the antenna and the injected gas flow rate was set, respectively, at 900 W and 3 SCCM.

The emission intensities for each magnetic field strength were measured using OES. In this measurement, the argon single ion emission line (434.8 nm) was selected since it has the maximum emission intensity among the prominent lines of the spectra in the wavelength range of 300–550 nm.

The results of the argon single ion line (434.8 nm) emission intensity, measured with varying intensities of the magnetic field are shown in Fig. 14, with error bars based on a 95% confidence interval from the fitting procedure. As observed in this figure, the
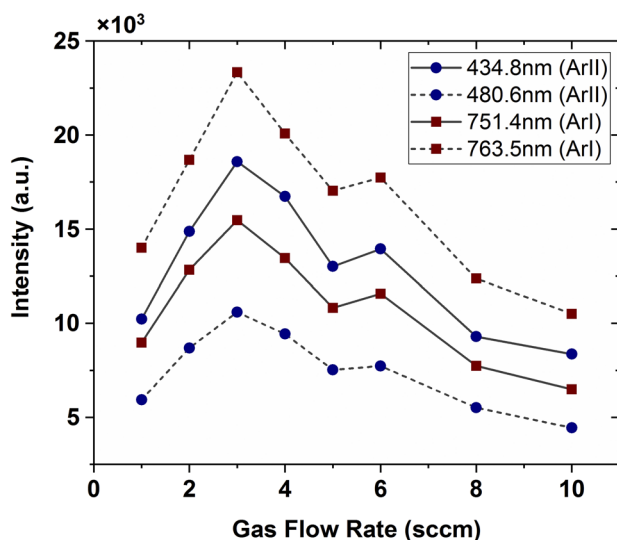
FIG. 14. The variations in the argon single ion line (434.8 nm) emission intensity vs the varying magnetic field intensities at 900 W RF power and 3 SCCM gas flow rate.

argon ion emission line increases with increase in the axial magnetic field intensity. This graph specially characterizes the magnetic field effect on the blue portion intensity of the obtained spectra. In addition, the linear dependence between the magnetic field strength and 434.8 nm emission line intensity suggests that the H-mode to W-mode coupling transition occurs for the magnetic field strengths below 100 mT as a discontinuity in the 434.8 nm emission intensity would be expected during this transition from the results presented in Figs. 9(a), 9(c), and 11.

V. CONCLUSION

An industrial helicon plasma source (AHPS-II) for material processing applications has been designed and developed in the helicon plasma laboratory of AUT. A photographic technique by using polaroid filters was accomplished for the m = +1 and m = −1 helicon mode confirmations of AHPS-II. It has been shown that the reddish color of the plasma was changed and the blue core appeared when the plasma was magnetized due to the external magnetic field and the RF power increased to 400 W in the 3 SCCM argon flow rate. In addition, the plasma ionization process from the H-mode to the W-mode was investigated by the OES method using a collimator setup. Based on spectral measurements, the intensity of the argon ion emission line increases as the RF power delivered to the antenna and, hence, to the plasma is increased. The argon single and neutral ion line emission intensities in the wavelength range of 400–450 nm and 800–850 nm were, respectively, compared for the ICP, m = −1, and m = +1 modes of operation. In the wavelength range of 800–850 nm, the argon neutral ion emission intensities drop by a factor of 2.27 ± 0.03 as the magnetic field was turned on in the m = −1 mode direction. In addition, the intensity of these ions under the same operational conditions decreases by a factor of 1.38 ± 0.02 when the magnetic field direction was changed for the m = +1 mode excitation. In addition, the intensity line ratio for the argon single ions in the wavelength range of 400–450 nm increases by factor of

FIG. 13. The variation in the argon single and neutral ion line (ArII: 434.8 nm, 480.6 nm and ArI: 751.4 nm, 763.5 nm) emission intensities vs argon flow rates for m = +1 helicon mode at 300 mT magnetic field intensity and 900 W RF power.

116.5 ± 7.3 and 2.03 ± 0.07, respectively, for the transition from ICP to m = −1 and m = −1 to m = +1 modes of operation. Based on the spectral measurements of different gas flow rates ranged from 1 SCCM to 10 SCCM, at 900 W RF power and 300 mT magnetic field intensity, there is an optimized 3 SCCM mass flow rate in which the argon single and neutral ion line emission intensities for 2 SCCM and 4 SCCM gas flow rates, respectively, decreases 20% and 12%. Finally, it was observed at 900 W RF power and 3 SCCM gas flow rate that the argon single ion emission intensity has a linear dependence on the variations in the magnetic field strength, indicating coupling transition from the H-mode to the W-mode for the magnetic field intensities lower than 100 mT. The ion beam extraction from the AHPS-II for material processing applications and experimental measurements of the beam optical characteristics such as the beam current and profile is the topic of our future work. The construction of a novel triode extraction system and its simulations were presented in Ref. 10, which is one of our future plans in the way of the construction of an industrial helicon ion source.

ACKNOWLEDGMENTS

DATA AVAILABILITY

The data that support the findings of this study are available within the article.

REFERENCES

[1] C. R. Legendy, "Macroscopic theory of helicons," Phys. Rev. **135**, A1713 (1965).

[2] F. F. Chen, "Plasma ionization by helicon waves," Plasma Phys. Controlled Fusion **33**, 339 (1991).

[3] R. W. Boswell, "Plasma production using a standing helicon wave," Phys. Lett. A **33**, 457 (1970).

[4] A. R. Ellingboe and R. W. Boswell, "Capacitive, inductive and helicon-wave modes of operation of a helicon plasma source," Phys. Plasmas **3**, 2797 (1996).

[5] R. Boswell, "A study of waves in gaseous plasmas," Ph.D. thesis, Flinders University, Adelaide, Australia, 1970.

[6] P. Zhu and R. W. Boswell, "Ar II laser generated by Landau damping of whistler waves at the lower hybrid frequency," Phys. Rev. Lett. **63**, 2805 (1990).

[7] P. Zhu and R. W. Boswell, "A new argon-ion laser based on an electrodeless plasma," J. Appl. Phys. **68**, 1981 (1991).

[8] A. W. Degeling, C. O. Jung, R. W. Boswell, and A. R. Ellingboe, "Plasma production from helicon waves," Phys. Plasmas **3**, 2788 (1996).

[9] J. Scharer, A. Degeling, G. Borg, and R. Boswell, "Measurements of helicon wave propagation and Ar II emission," Phys. Plasmas **9**, 3734 (2002).

[10] M. Khoshhal, M. Habibi, and R. Boswell, "Development of a new high-current triode extraction system for helicon ion source: Design and simulation," Laser Part. Beams **36**, 477 (2018).

[11] C. S. Corr and R. W. Boswell, "High-beta plasma effects in a low-pressure helicon plasma," Phys. Plasmas **14**, 122503 (2007).

[12] E. E. Scime, P. A. Keiter, M. M. Balkey, R. F. Boivin, J. L. Kline, M. Blackburn, and S. P. Gary, "Ion temperature anisotropy limitation in high beta plasmas," Phys. Plasmas **7**, 2157 (2000).

[13] A. J. Perry, D. Vender, and R. W. Boswell, "The application of the helicon source to plasma processing," J. Vac. Sci. Technol., B **9**, 310 (1991).

[14] F. F. Chen, "Permanent magnet helicon source for ion propulsion," IEEE Trans. Plasma Sci. **36**, 2095 (2008).

[15] C. Charles, "Plasmas for spacecraft propulsion," J. Phys. D: Appl. Phys. **42**, 163001 (2009).

[16] O. V. Batishchev, "Minihelicon plasma thruster," IEEE Trans. Plasma Sci. **37**, 1563 (2009).

[17] Y. Sakawa, T. Takino, and T. Shoji, "Control of antenna coupling in high-density plasma production by m = 0 helicon waves," Appl. Phys. Lett. **73**, 1643 (1998).

[18] R. W. Boswell, "Very efficient plasma generation by whistler waves near the lower hybrid frequency," Plasma Phys. Controlled Fusion **26**, 1147 (1984).

[19] R. Bowers, C. Legendy, and F. E. Rose, "Oscillatory galvanomagnetic effect in metallic sodium," Phys. Rev. Lett. **7**, 339 (1961).

[20] T. Shoji, Y. Sakawa, S. Nakazawa, K. Kadota, and T. Sato, "Plasma production by helicon waves," PIasma Sources Sci. Technol. **2**, 5 (1993).

[21] D. Melazzi and V. Lancellotti, "A comparative study of radiofrequency antennas for Helicon plasma sources," Plasma Sources Sci. Technol. **24**, 025024 (2015).

[22] D. G. Miljak and F. F. Chen, "Helicon wave excitation with rotating antenna fields," Plasma Sources Sci. Technol. **7**, 61 (1998).

[23] S. Shinohara, "Helicon high-density plasma sources: Physics and applications," Adv. Phys.: X **3**, 1420424 (2018).

[24] F. F. Chen, *High Density Plasma Sources* (Elsevier, 1995), Chap. I.

[25] I. D. Sudit and F. F. Chen, "Discharge equilibrium of a helicon plasma," Plasma Sources Sci. Technol. **5**, 43 (1996).

[26] M. Celik, "Spectral measurements of inductively coupled and helicon discharge modes of a laboratory argon plasma source," Spectrochim. Acta, Part B **66**, 149 (2011).

[27] E. E. Scime, A. M. Keesee, and R. W. Boswell, "Mini-conference on helicon plasma sources," Phys. Plasmas **15**, 058301 (2008).

[28] C. M. Franck, O. Grulke, and T. Klinger, "Mode transitions in helicon discharges," Phys. Plasmas **10**, 323 (2003).

[29] B. Soltani and M. Habibi, "Development of a helicon plasma source for neutral beam injection system of the Alborz tokamak," J. Fusion Energy **36**, 152 (2017).

[30] M. A. Lieberman and R. W. Boswell, "Modeling the transitions from capacitive to inductive to wave-sustained rf discharges," J. Phys. IV **08**, Pr7 (1998).

[31] F. F. Chen and D. Arnush, "Generalized theory of helicon waves. I. Normal modes," Phys. Plasmas **4**, 3411 (1997).

[32] I. V. Kamenski and G. G. Borg, "An evaluation of different antenna designs for helicon wave excitation in a cylindrical plasma source," Phys. Plasmas **3**, 4396 (1996).

[33] S. C. Thakur, C. Brandt, L. Cui, J. J. Gosselin, and G. R. Tynan, "Formation of the blue core in argon helicon plasma," IEEE Trans. Plasma Sci. **43**, 2754 (2015).

[34] F. F. Chen and R. W. Boswell, "Helicons-the past decade," IEEE Trans. Plasma Sci. **25**, 1245 (1997).

[35] S. Shinohara, Y. Miyauchi, and Y. Kawai, "Dynamic plasma behaviour excited by m = + or −1 helicon wave," Plasma Phys. Controlled Fusion **37**, 1015 (1995).

[36] T. Enk and M. Krämer, "Radio frequency power deposition in a high-density helicon discharge with helical antenna coupling," Phys. Plasmas **7**, 4308 (2000).

[37] Y. M. Aliev and M. Krämer, "Effect of the radial plasma nonuniformity on the propagation of guided m = +1 and m = −1 modes in helicon discharges," Phys. Plasmas **23**, 103505 (2016).

[38] NIST Atomic Spectra Database, 2019, http://www.physics.nist.gov/PhysRefData/ASD/index.html.

[39] S. M. Tysk, C. M. Denning, J. E. Scharer, and K. Akhtar, "Optical, wave measurements, and modeling of helicon plasmas for a wide range of magnetic fields," Phys. Plasmas **11**, 878 (2004).

[40] A. Shabshelowitz, "Study of RF plasma technology applied to air-breathing electric propulsion," Ph.D. thesis, University of Michigan, 2013.

[41] X. M. Guo, J. Scharer, Y. Mouzouris, and L. Louis, "Helicon experiments and simulations in nonuniform magnetic field configurations," Phys. Plasmas **6**, 3400 (1999).

[42] J. P. Rayner and A. D. Cheetham, "Helicon modes in a cylindrical plasma source," Plasma Sour. Sci. Technol. **8**, 79 (1999).

[43] M. Krämer, "Propagation and damping of m = +1 and m = −1 helicon modes in an inhomogeneous plasma column," Phys. Plasmas **6**, 1052 (1999).

[44] B. Clarenbach, M. Krämer, and B. Lorenz, "Spectroscopic investigations of electron heating in a high-density helicon discharge," J. Phys. D: Appl. Phys. **40**, 5117 (2007).

[45] M. A. Hassouba and N. Dawood, "A comparative spectroscopic study on emission characteristics of DC and RF discharges plasma using different gases," Life Sci. J. **11**, 656 (2014).

[46] N. Sinenian, "Propulsion mechanisms in a helicon plasma thruster," M.S. thesis, Massachusetts Institute of Technology, 2008.